

CARAT: Client-Side Adaptive RPC and Cache Co-Tuning for Parallel File Systems

Md Hasanur Rashid¹, Nathan R. Tallent², Forrest Sheng Bao³, Dong Dai¹

¹University of Delaware, ²Pacific Northwest National Laboratory, ³Iowa State University

Email: {mrashid,dai}@udel.edu, tallent@pnnl.gov, forrest.bao@gmail.com

Abstract—Tuning parallel file system in High-Performance Computing (HPC) systems remains challenging due to the complex I/O paths, diverse I/O patterns, and dynamic system conditions. While existing autotuning frameworks have shown promising results in tuning PFS parameters based on applications’ I/O patterns, they lack scalability, adaptivity, and the ability to operate online. In this work, focusing on scalable online tuning, we present CARAT, an ML-guided framework to co-tune client-side RPC and caching parameters of PFS, leveraging only locally observable metrics. Unlike global or pattern-dependent approaches, CARAT enables each client to make independent and intelligent tuning decisions online, responding to real-time changes in both application I/O behaviors and system states. We then prototyped CARAT using Lustre and evaluated it extensively across dynamic I/O patterns, real-world HPC workloads, and multi-client deployments. The results demonstrated that CARAT can achieve up to 3× performance improvement over the default or static configurations, validating the effectiveness and generality of our approach. Due to its scalability and lightweight, we believe CARAT has the potential to be widely deployed into existing PFS and benefit various data-intensive applications.

I. INTRODUCTION

Today, high-performance computing (HPC) systems increasingly support data-intensive scientific applications [1–5]. These applications typically execute across a large number of computing nodes, issuing concurrent I/O requests to multiple remote storage servers. As illustrated in Figure 1, the I/O client, which runs within each computing node as part of the parallel file system (PFS) client library, translates application-level I/O requests into individual I/O RPCs over the network, ultimately reaching different storage servers within the PFS. These concurrent I/O clients, operating rigidly according to their predefined parameter settings, can easily cause mismatches among various components along the long I/O paths at runtime, leading to suboptimal performance. For example, an I/O client might attempt to send excessive I/O requests to an already saturated network or storage server causing high contention and degraded performance, or it may fail to construct sufficient I/O RPCs promptly despite available network capacity [6].

Essentially, at runtime, the I/O clients must balance two key aspects that significantly impact I/O performance: (1) the rate at which they generate I/O RPCs, and (2) the rate at which these RPCs are transmitted and served. These aspects can be further summarized into two fundamental factors: the *local cache/buffer status* and the *communication performance*. The state of the local buffer or cache, including its total capacity and current utilization, dictates how application-generated I/O

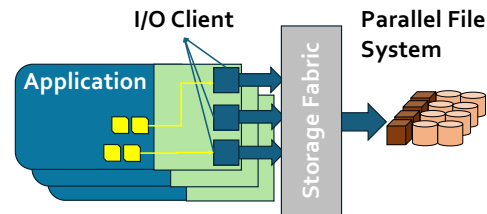


Fig. 1. The I/O clients serve individual I/O request.

requests are aggregated into locally buffered operations or immediately issued as network I/O RPCs. Meanwhile, the condition of the communication layer, characterized by (1) the number of RPCs that can be sent concurrently, (2) their sizes, and (3) the rate at which remote storage servers process them, determines how efficiently those network I/O RPCs are served. These two factors, like producers and consumers, must operate in coordination to achieve optimal performance. It has been shown that tuning relevant configurations, such as cache/buffer sizes or the number of concurrent network channels, can significantly enhance the I/O performance [7–9]. For instance, Bez et al. demonstrated proper configurations can achieve a 6.8× speedup for the OpenPMD application and a 7.9× speedup for the FLASH-IO benchmark on the Cori and Summit supercomputers [10].

Most of existing efforts try to find optimal configurations via modeling application I/O patterns and leveraging these patterns to explore configuration spaces. For instance, one may have larger number of RPCs that can be concurrently sent for large sequential I/O patterns because they typically benefit from more parallel network channels, whereas small random I/O patterns may benefit from reducing the maximal size of RPCs, which facilitates smaller RPCs for better network utilization. For instance, Behzad et al. proposed a pattern-driven I/O tuning approach using genetic algorithms guided by I/O pattern prediction models [11]. Other studies have explored different search strategies based on modeled I/O patterns [12–14]. Recent methods, such as CAPES [15] and AIOC2 [16], have integrated deep reinforcement learning (DRL) for end-to-end I/O parameter tuning, implicitly modeling I/O patterns through reinforcement learning agents.

However, *understanding application I/O patterns and then configuring I/O clients accordingly* faces practical challenges. HPC applications’ I/O patterns arise from the collective behaviors of all ranks. Accurately detecting them is inherently

difficult, and effectively using these detected patterns to navigate extensive configuration spaces further complicates the task. The accuracy of I/O pattern detection can be substantially impaired by factors such as changing application I/O behaviors and unpredictable interference from concurrent applications [17–19]. Models that demonstrate good performance often rely heavily on global runtime metrics, such as CAPES [15] and AIOC [16], resulting in high overhead for metric collection and model training. Due to such heavy overhead, ‘best configurations’ are frequently simplified to a single set of values to be uniformly applied across all I/O clients, even if they may be from different computing nodes and interact differently with storage servers or network channels [15, 16, 20–22]. Such simplifications lead to unstable and suboptimal performance, as demonstrated in subsequent evaluation sections.

In this study, we propose a radically different approach. Instead of relying on modeling applications’ global I/O patterns, we narrow our focus directly on the individual I/O clients on the computing nodes. Specifically, we tune configurations to alter behaviors of each I/O client purely *based on locally observable metrics instead of global application I/O patterns*. Leveraging machine learning models, multiple independent tunable I/O clients on different computing nodes can make timely decisions to respond effectively to changing workloads and collectively to global storage system conditions, resulting in improved I/O performance for the entire application.

The benefits of tuning individual I/O clients are threefold. First, it is extremely lightweight, allowing immediate response to changing I/O patterns or even short-term interferences on the server side. Second, each client is independently tuned, enabling the assignment of optimal configurations per client instead of a single compromised configuration for all clients. Lastly, by treating global network/storage systems as external environments and considering their real-time responses to previous requests, the approach can effectively react to global system status. We argue that, although the metrics are collected locally, they can implicitly reflect critical information for conducting global tuning. Specifically, they can reflect: 1) how I/O operations are constructed through buffering/caching mechanisms, 2) how these operations are sent as network RPCs, and 3) how global network/storage systems respond to previous RPC requests. Manually interpreting such implicit information is difficult, we can leverage machine learning to learn it.

To validate such an idea, in this study, we designed and prototyped **Client-side Adaptive RPC** and **cAche co-Tuning (CARAT)** framework for co-tuning *client-side RPC and cache* of Lustre, one of the most popular parallel file systems used in modern HPC clusters [23]. Running on each Lustre I/O client, CARAT samples client-local metrics and applies a learned policy to adjust the RPC window, in-flight concurrency, and dirty-cache size online. Tuning decisions are enacted immediately and periodically, enabling rapid adaptation to changing I/O patterns of application and contention cluster-wide. We then extensively evaluated CARAT across various scenarios, including sequential/random and dynamic patterns, single- and multi-client runs, and interference conditions,

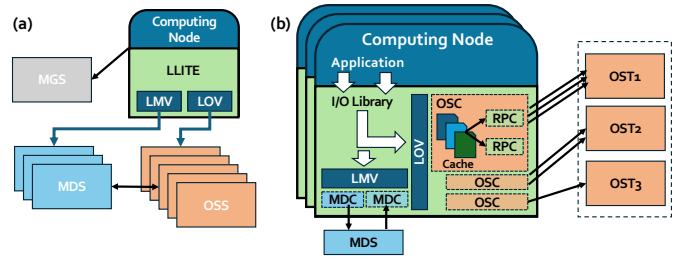


Fig. 2. (a) The overall architecture and (b) the detailed I/O path of Lustre.

CARAT improves performance by up to $3\times$ over default Lustre settings. Our contributions are:

- A ML-guided system for *client-side RPC and cache co-tuning* leveraging client-local observations.
- A client-side observability model that enables online, per-client decisions without cluster-wide instrumentation.
- Comprehensive evaluations demonstrating up to $3\times$ improvement over default configuration across diverse scenarios.

The rest of the paper is organized as follows: In §II, we discuss relevant backgrounds of Lustre file system and key ideas behind some of CARAT’s design choices. In §III, we present the architecture of CARAT in detail. We present the extensive experimental results in §IV. We highlight the relevant works to our study in §V, conclude the paper and discuss the future work in §VI.

II. BACKGROUND AND KEY IDEAS

In this section, we first use Lustre [23] as an example to illustrate how the local cache and network RPC mechanisms interact and jointly influence I/O performance. We then discuss how local metrics and machine learning models can be leveraged to capture such complex interactions. Finally, we briefly discuss the applicability of our approach to other parallel file systems.

A. Lustre RPC and Caching Mechanisms

Figure 2(a) first illustrates the overall architecture of Lustre which comprises one management server (MGS), one or more metadata servers (MDSs), and multiple object storage servers (OSSs). The management server (MGS) is lightweight and typically deployed alongside one of the metadata servers (MDSs). On a computing node, I/O requests issued by applications, such as `open` or `read`, are managed by the I/O Client library. Within this library, Lustre Lite (LLITE) acts as a bridge between application and the underlying Lustre infrastructure, represented by the Lustre Object Volume (LOV) and the Lustre Metadata Volume (LMV).

Figure 2(b) further shows how I/O requests are processed by the I/O clients. For data accesses, the I/O requests are handled by the LOV component, which establishes multiple Object Storage Client (OSC) interfaces, each corresponding to one Object Storage Target (OST) on OSS. Each OSC interface is responsible for formulating RPCs and managing RPC communications directed to a specific OST. Similarly, the

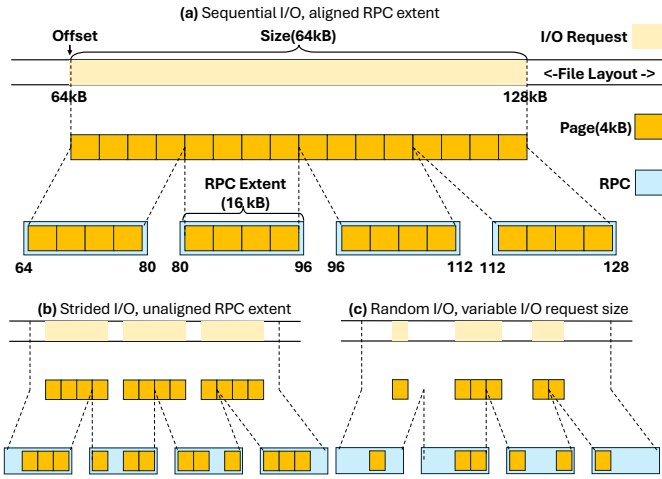


Fig. 3. An illustration of how I/O requests are split into pages and aggregated into fixed-size RPC extents.

Lustre Metadata Volume (LMV) component manages metadata accesses to metadata targets (MDTs) on MDSs via the Metadata Client (MDC) interface. Together, OSC and MDC play the role of *I/O Client* as described earlier.

During I/O operations, the I/O Client will utilize local *dirty-page cache* to buffer individual writes, which will be aggregated into RPCs to be sent to the remote OSTs. RPCs are built based on building a fixed-size *RPC extent* (size controlled by `osc.*.max_pages_per_rpc`), which includes a consecutive group of pages targeting the same OST. RPCs will be mature and dispatched via network channels when one of following events occur: 1) the extent fills, 2) a kernel wait threshold expires, or 3) cache pressure (*cache-waiters*) forces a flush. How many RPCs can be sent out concurrently is bounded by *RPCs in flight* (controlled by `osc.*.max_rpcs_in_flight`).

Figure 3(a) details how the ideal case works. It shows a 64 kB request issued at a 64 kB offset gets split into 4 kB pages and packed into 16 kB RPC extents. In this example, because the request is sequential and aligned to page and extent boundaries, all extents are filled and triggering the resulting RPCs to be issued as soon as an RPC channel is available.

Complex coordination between RPC and Caching. In practice, the buffering and RPC formation could introduce various I/O performance bottlenecks under diverse I/O patterns and dynamic contention as exemplified below.

a) Under-filled extents and cache fragmentation. Irregular, unaligned, or random I/O requests may not be able fill RPC extents in time. These partially filled extents will be held in cache, occupying space, blocking admission of new pages, and delaying sending out I/Os. Figure 3(b) and (c) show examples of such cases, where unaligned strided or random small I/Os are organized into different extents. These partially filled extents will not be sent out as a new RPC until a timeout event happens, which delays the existing I/Os while blocking the new I/Os.

b) Server-side congestion under contention. On the other hand, if I/O Clients are able to fill the extents fast and construct RPCs radically, these bursts of small RPCs can overwhelm

TABLE I
SUMMARY OF TUNABLE PARAMETERS FOR LUSTRE CLIENTS

Category	Parameter	Description
RPC	<code>osc.*.max_pages_per_rpc</code>	Max size of a single data RPC.
	<code>osc.*.max_rpcs_in_flight</code>	Max number of concurrent data RPCs allowed.
Caching	<code>osc.*.max_dirty_mb</code>	Max dirty-page cache limit for data I/O.

the remote storage server’s I/O queues, significantly increasing queuing delay and degrading throughput. Worse, the congestion could further amplify the impacts of premature dispatch and insufficient extent filling.

c) Cache-limit throttling. The size of the dirty caches also impacts the I/O behaviors. The conservative, low dirty-cache limits will send out immature RPCs earlier, which restrict coalescing and cap throughput. But, overly large dirty-cache limits can buffer lots of I/Os, leading to bursty flush storms that overwhelm the backend during transient write spikes.

As these examples show, the interactions between caching and RPC are complicated and impacted by various factors, such as workloads, server status, and network contentions. In practice, there may be additional RPC classes (e.g., cache-waiters or lock-conflict related) further complicating the coordination to optimize I/O performance. In this study, we propose to leverage machine learning methods to learn such complex relationships. Model details are in § III-C

B. Tunable Parameters for RPC and Caching

In this study, we focus on two categories of parameters to tune, as Table I summarizes. Note that, while metadata requests follow similar RPC and cache structure, in this work we focus on data-path behavior and do not tune metadata parameters.

We selected these parameters for several reasons. First, they are specific to the I/O clients, allowing them to be tuned independently at each I/O client (*independent*). Second, these parameters can be dynamically adjusted and will take effect at runtime, making them ideal for validating our approach (*adaptive*). In contrast, many Lustre parameters, such as *stripe count* and *stripe size*, cannot be modified once set, and thus are excluded from our considerations. Our tuning can complement these tuning efforts at runtime. For instance, CARAT can further enhance I/O performance after the optimal stripe count and stripe size have been determined.

It is also important to highlight that, although both RPC parameters and caching parameters take effect at runtime, their impacts manifest at different rates. Changes to RPC parameters affect I/O operations immediately, influencing all newly constructed RPCs. Although existing RPCs already in flight remain unaffected, they typically complete within microseconds; therefore the delay is negligible. On the other hand, changes to caching parameters require more time to propagate. For instance, increasing cache size may not show performance changes until sufficient I/O arrives to take

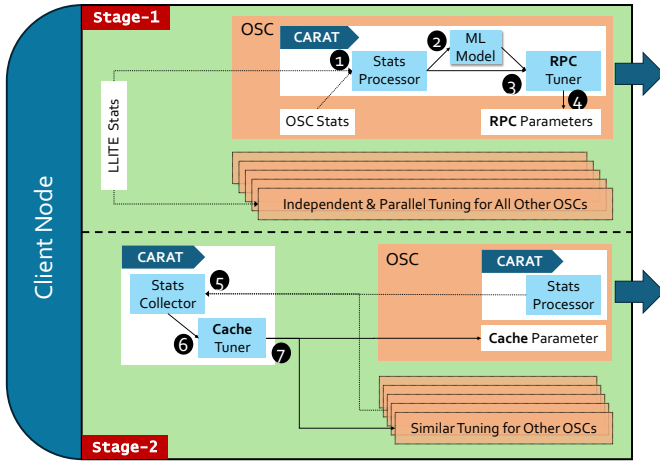


Fig. 4. Architecture of the CARAT framework.

advantage of increased cache size. This discrepancy makes it challenging to determine whether performance changes are due to adjustments in RPC or caching parameters. To address this, CARAT employs a two-phase tuning approach, handling these parameters separately. The details will be discussed in § III-A. C. *Applicability to Other PFS*

Our approach targets a rather general design principle in parallel file systems: buffered, aggregated small I/Os served via network RPCs. Such a practice is widely seen and essential for better I/O performance in networked FS. Hence, we argue the method can be applied widely. For example, Network File System (NFS) [24] buffers and issues I/O via RPCs and exposes analogous tunables. Parameters such as `nfs4_max_transfer_size` (max transfer size) and `tcp_slot_table_entries` (max outstanding RPCs) play roles similar to `max_pages_per_rpc` and `max_rpcs_in_flight`. Client-local tools (e.g., `nfsiostat`) provide the metrics needed for online decisions, suggesting our mechanism can be adapted where similar client-side RPC and caching behaviors exist.

III. DESIGN AND IMPLEMENTATION

In this study, we implemented a CARAT prototype based on the Lustre file system, which operates autonomously as part of the Lustre I/O client. Figure 4 illustrates the overall architecture of CARAT, divided into two stages.

The *Stage-1* begins from the system stats processor component (1) probes the local-level statistics from I/O client at user-defined intervals. These statistics are then preprocessed to extract defined metrics (defined in § III-B). We then create the snapshots incorporating these metrics for each I/O client. The processed snapshots (2) are then fed into the local ML model component, which generates a probability distribution across the configuration space. This distribution assesses the likelihood of each configuration achieving performance improvement if applied. Armed with the probability distribution and the snapshot for each I/O client, the RPC tuner (3) component determines the optimal RPC configuration and applies it (4). This whole process repeats at each interval and continues

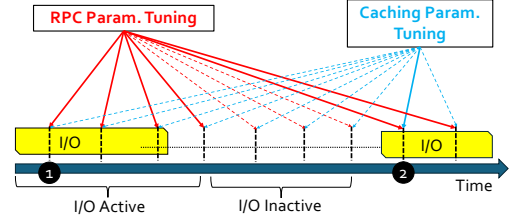


Fig. 5. The Two-stage tuning strategy in CARAT.

throughout the duration of CARAT operation on the client, ensuring continuous optimization.

The *Stage-2* happens concurrently with *Stage-1* at the beginning of I/O active stage following the I/O inactive stage. It focuses on tuning the cache parameters. The stats collector component (5) gathers statistics from the stats processor of each I/O client. It then forwards the collected data to the cache tuner component (6), which determines the appropriate cache limit for each I/O client based on the observed metrics and applies the corresponding parameter changes (7).

A. Two-Stage Tuning Principle

CARAT introduces this two-stage tuning strategy to tune RPC parameters and caching parameters separately. Figure 5 shows how the two-stage tuning strategy works in CARAT. We consider each application execution would consist of two stages: *I/O Active* and *I/O Inactive*, which can be easily differentiated from the I/O client by observing how many I/O requests were sent to the I/O library during last observation window (e.g., 1 second). If there are I/O requests (yellow part), then we consider to be in the I/O active stage. Otherwise, we define it as the I/O inactive stage.

During I/O active stage, we only perform RPC tuning based on the user-defined tuning frequency. Since changes to RPC parameters impact the I/O performance instantly, we will be able to observe how previous tuning impacts the system by monitoring the metrics in real-time. Using the most recent local metrics, the tuner makes new tuning decision at each observation (solid arrows, marked 1 in Figure 5). During I/O inactive stage, there is no actual I/O. We disable RPC parameter tuning during this stage since there exists no RPC transfers.

We tune caching parameter only at the end of the I/O inactive stage, that is, at the first observed time-point when I/O activity resumes (solid arrow, marked as 2 in Figure 5). At this point, the tuner uses collected metrics during *I/O active stage* to assess whether the previous caching configuration is appropriate and adjusts them as needed. We select this time point to tune caching parameters because after the period of I/O inactive stage (>1 second), the impacts of the previous caching configuration should have well faded, making the impacts of the new caching configuration more easily observed.

B. I/O Client Local Metrics

Obtaining low-level client-side metrics is crucial for CARAT. The metrics must (i) expose application I/O behavior and the client’s view of network/server state, (ii) scale with negligible

TABLE II
SUMMARY OF DESIGNED CLIENT-SIDE LOCAL METRICS AND THEIR CHARACTERISTICS

Metric Name	RPC Page Utilization	RPC Channel Utilization	Unit Page RPC Latency	Data Transfer Volume	Dirty Cache Utilization	Estimated Cache Update
<i>Used For:</i>	RPC & Cache tuning	RPC & Cache tuning	RPC tuning	RPC & Cache tuning	RPC & Cache tuning	RPC tuning
<i>Meaning:</i>	Ratio of average to max pages per RPC	Ratio of average to max RPCs in flight	Avg. latency per page for RPCs	Total data transferred through RPCs	Dirty cache usage ratio	Estimated data update in cache
<i>Captures Locally:</i>	RPC formulation quality	RPC parallelism, actual vs. allowed RPCs	-	Volume of transferred data	Current buffer utilization	Local cache updates, reduced RPC needs
<i>Reflects Globally:</i>	-	Network contention, server grants for RPCs	Network latency, impact of server I/O load	End-to-end throughput, total RPC traffic	Limited allocation due to server overload	-

overhead, and (iii) be robust enough for online learning and control. Unlike prior pattern-centric approaches [15, 16, 20], we rely on scalable, client-local metrics that reflect application and system effects (§ IV); we also pre-process raw counters into stable, normalized features suitable for learning. All metrics are computed separately for `read` and `write` because the paths differ (e.g., dirty-page vs. readahead). Table II summarizes the set; we describe each briefly below.

RPC Page Utilization. This is the ratio of average to maximum pages per RPC. It reflects how well fixed-size extents are filled before dispatch, integrating spatial/temporal access patterns (sequential/strided/random, bursty vs. steady), available client cache, and object striping. Persistently low values indicate under-filled extents (more small RPCs, delayed coalescing), whereas high values suggest effective aggregation.

RPC Channel Utilization. Defined as the ratio of average to maximum *RPCs in flight*, this metric captures realized parallelism relative to configured limits. It decreases when RPC formation stalls (e.g., sparse arrivals, cache pressure) or when server-side throttling reduces concurrency; it may exceed nominal caps due to priority issuance (e.g., cache-waiters or lock-related RPCs), signaling exceptional drain behavior.

Unit Page RPC Latency. Average latency per page transferred, which normalizes out batch size and concurrency. By factoring out RPC size and channels, this metrics reflects network and server conditions (e.g., queue buildup, transient congestion) rather than batching artifacts, thus more stable across pattern shifts.

Data Transfer Volume. Total bytes transferred via RPCs during the interval (e.g., 1 s). It provides a direct throughput signal and, together with latency/utilization, distinguishes “busy and healthy” from “busy and congested” conditions, stabilizing policy updates.

Dirty Cache Utilization. Fraction of the dirty-page cache currently in use. Rising pressure indicates backlog (RPC issuance not draining writes fast enough) or a phase with heavy write arrival; in conjunction with page/channel utilization it reveals whether limited headroom is preventing effective coalescing.

Estimated Cache Update. An estimate of bytes updated in-place within the dirty cache (e.g., in-place or small random

writes that overwrite cached regions) rather than sent immediately. We approximate it from per-client write shares on a node minus observed RPC drain and cache delta, avoiding per-request tracing while still identifying phases where enlarging cache headroom materially improves performance.

Metrics on Changes. For all metrics, CARAT also tracks short-term deltas between consecutive intervals. These trends highlight emerging contention or recovery and let the controller react promptly without overcorrecting to transient spikes.

C. ML Model for RPC Parameter Tuning

To accurately capture the characteristics of client-local metrics, we utilize ML models to comprehend how the current values of client metrics might influence I/O and how a particular configuration would impact the performance accordingly.

Rather than naively forecasting the exact performance value for a configuration, which is highly dependent on the cluster hardware, we re-map the problem to a classification task. Specifically, the ML model will only determine whether a given configuration will lead to a better I/O performance than the current configuration. We consider ‘better’ as an improvement beyond a set threshold (in our case, 15%) considering possible noises. If the model predicts a greater than 80% probability of improvements, it classifies the outcome for that configuration as positive (one); otherwise, it is negative (zero). The probability threshold defined here (80%) is to ensure we have a good set of candidates with a high chance of better performance and avoid selecting opportunistic choices with low confidence in performance improvement.

To formally define the ML models, let \mathbf{s}_t represent a vector of client-local metrics at timestep t . A short history of system performance of k timesteps is thus $\mathbf{H}_t = [\mathbf{s}_{t-k}, \mathbf{s}_{t-k+1}, \dots, \mathbf{s}_t]$. We further denote the tunable parameters of the system at timestep t as θ_t , which is also a vector. The goal of a ML model here is to find a function f that predicts the likelihood that the setting θ_t will result in a performance improvement over a threshold ϵ (e.g., 15%) in the next timestep, thus $f(\theta_t, \mathbf{H}_t) = \mathbb{E}[s_{t+1}/s_t > 1 + \epsilon]$ where \mathbb{E} is expectation.

In our study, we experimented multiple ML architectures, including support vector machines (SVMs) [25], neural networks (NNs) [26], and gradient boosting decision trees (GBDTs) [27].

Algorithm 1: RPC Parameter Tuning Algorithm

Data: RPC space Θ , system history \mathbf{H}_t , op type o , current config $\theta_t = \{\theta_t^1, \theta_t^2\}$, threshold τ , weights α, β

Result: Optimized config θ^*

- 1 $S \leftarrow \{\theta \in \Theta \mid f(\theta, \mathbf{H}_t) > \tau\}$;
 - 2 Normalize S using MinMax normalization;
 - 3 $\theta^* \leftarrow \arg \max_{\theta \in S} (o =$
‘Write’ ? WriteScore(θ, \mathbf{H}_t) :
ReadScore(θ, \mathbf{H}_t));
 - 4 **Function** WriteScore(θ, \mathbf{H}_t):
 - 5 $\lfloor f(\theta, \mathbf{H}_t) \cdot (1 + \beta \sum \theta) \rfloor$;
 - 6 **Function** ReadScore(θ, \mathbf{H}_t):
 - 7 $\lfloor f(\theta, \mathbf{H}_t)(1 + \alpha \theta^1) + \theta^2 \rfloor$;
-

For NNs, we experimented, Fully-Connected NNs (FC-NNs), vanilla Recurrent Neural Networks (RNNs) [28], and Temporal Convolutional Networks (TCNs) [29]. Because SVMs, GBDTs, and FC-NNs do not have the ability to take data sequentially or iteratively, \mathbf{H}_t is flattened into a 1-D vector $s_{t-k} \oplus s_{t-k+1} \oplus \dots \oplus s_t$ before being fed into the said ML architectures. For RNNs and TCNs, the vector $s_{i \in [t-k..t]}$ is fed into the NN each time. As to be shown later in § IV-C, GBDTs are the most suitable architecture for our problem and $k = 1$ provides the best value.

We train the model by sweeping client configurations; after each change, we measure the next interval’s performance and label the sample 1 if improvement $> 15\%$, else 0. At runtime, each client periodically queries the model with \mathbf{H}_t and candidate θ_t ; the model returns the probability of being 1.

We train separate models for read and write operations. This differentiation stems from observing distinct approaches the Lustre employs in handling these operations. By training separate models, we can better predict the likelihood of I/O performance improvement based on client-local metrics and given configuration. In the next section, we discuss how the observation of client-local metrics and insights generated from the ML model enable us to decide the tuning actions on the parameters.

D. RPC Tuner: Conditional Score Greedy

As described earlier, we adopt separate tuning strategies for read and write operations because reads and writes exercise different components of the Lustre I/O path (e.g., buffering/writeback and lock/cache pressure for writes versus request parallelism for reads), leading to different performance sensitivities. CARAT maintains two trained models (read-focused and write-focused) and selects the model at each observation period based on the dominant observed I/O volume (Data Transfer Volume, in bytes): if read volume dominates, it uses the read model; otherwise it uses the write model. The ML model assigns a probability to each input configuration, providing an approximation of which configurations are likely to enhance I/O performance. However, identifying the optimal configuration from these high-probability options is nontrivial.

At the beginning, we intuitively utilized the *Greedy Tuning* strategy, which picks the parameter configuration predicted with the highest probability to improve the performance. However, we quickly noticed that the high probability does not always lead to the optimal configuration. Instead, it likely picks the safer configuration with little improvement. We then improved the pure greedy strategy to *Epsilon Greedy*, by introducing a small ϵ value to randomly select the highest probability configuration (exploitation) or pick a random configuration (exploration). The overall performance improves. But it also introduces long delays and high variances in tuning. In this study, we introduce a *Conditional Score Greedy* approach that (i) filters candidate configurations using the model probability and a threshold τ , and (ii) ranks only the retained candidates using a priority score that combines the probability with a lightweight notion of parameter “trend” (i.e., preference for configurations that are more likely to remain beneficial under future variations). Algorithm 1 outlines the tuning strategy.

For each configuration θ , the ML model will output the probability of improving the performance by at least 15%. If the probability is over a preset threshold τ , the corresponding θ is added to the set S for further consideration (line 1). We set τ as 0.8 in our experiment. Selecting the optimal θ as $\arg \max_{\theta} f(\theta, \mathbf{H}_t)$ reduces to pure greedy tuning, which prefers high probability, safe configurations. Thus, we add regularization terms to them (lines 5 and 7). These regularization terms bias selection toward candidates that are both high-confidence and sufficiently “progressive” (rather than minimally safe), which empirically reduces long exploration delays while avoiding unstable random exploration.

Specifically, we prioritize the larger values of the two selected parameters (‘RPC Window Size’ and ‘RPCs in Flight’) when several configurations can all improve the performance. This is because, in general, a larger RPC size would utilize network channels better and more RPCs in flight would transfer more data in parallel. Hence, they have a higher chance of being better configurations in the future. Of course, higher values alone certainly would lead to extremely bad performance, which necessitates the continuous tuning. To control this tradeoff, the score uses two hyper-parameters (α, β) that balance the importance of the candidate’s predicted probability versus the preference term over the θ values; in our experiments we set $\alpha = \beta = 0.5$ to provide a balanced gain–stability tradeoff.

E. Cache Tuner: Rule-based Heuristic

The Lustre file system buffers write data in a dirty page cache before sending it to servers. As discussed in § III-A, this cache helps absorb I/O bursts and supports higher volumes of RPC transmission. However, naively setting a high cache limit can trigger frequent data flushes and risk server overload during high concurrency across I/O clients, leading production HPC systems to restrict cache sizes. To address this, we propose a dynamic cache limit allocation in Algorithm 2, which leverages a subset of local metrics collected during RPC tuning to enable informed and adaptive allocation.

Algorithm 2: Cache Parameter Tuning Algorithm

Data: Global cache limit D_{max} , active I/O clients O_{act} , inactive I/O clients O_{inact} , write volume $V_w[o]$, max cache usage $U_{max}[o]$, max in-flight RPC volume $R_{max}[o]$, discrete values of cache $B = \{2^x\}; x=5..11, B_{min} = 2^5, B_{max} = 2^{11}$

Result: Final cache allocations for all I/O clients, D

```
1  $b(x) := \min\{b \in B : b \geq x\};$ 
2  $D[o] \leftarrow B_{min}$  for all  $o \in O_{inact};$ 
3  $budget \leftarrow D_{max}/|O_{act}|, V_{tot} \leftarrow \sum_{o \in O_{act}} V_w[o];$ 
4 if  $budget \geq B_{max}$  then
5   |  $D[o] \leftarrow B_{max}$  for all  $o \in O_{act};$ 
6 else
7   |  $D[o] \leftarrow$ 
8     |  $\max(b(U_{max}[o]), b(R_{max}[o]), b(D_{max} \cdot V_w[o]/V_{tot}))$ 
9     | for all  $o \in O_{act};$ 
8 return  $D$ 
```

The algorithm begins by assigning the lowest cache value to all I/O clients with no I/O activity (line 2). If the available cache exceeds the total that active I/O clients can maximally use, it assigns the maximum cache value to all active I/O clients (line 5). Otherwise, it considers three factors to determine each active I/O client’s cache allocation: (1) *maximum cache utilization*, reflecting I/O bursts absorbed by the cache; (2) *peak in-flight RPC volume*, indicating RPC bursts accommodated; and (3) *the proportion of write RPCs handled by the I/O client*. For each factor, the algorithm selects the nearest equal or higher discrete cache value and then assigns the maximum among these three (line 7). While this approach may cause limited overprovisioning, it is acceptable as it remains bounded and cache usage naturally decreases as data is flushed to the servers.

F. Stability Considerations for Decentralized Tuning

Client-side decentralized control enables scalable adaptivity, but it can also introduce stability risks, including *oscillation* (e.g., reacting to short-lived fluctuations in observed metrics) and *under-utilization* (e.g., many clients simultaneously “backing off” under shared contention). CARAT mitigates these risks through several design choices. First, it applies probability-based candidate filtering with a threshold τ (set to $\tau = 0.8$ in our experiments), considering an update only when the model indicates a sufficiently strong likelihood of meaningful improvement, thereby reducing sensitivity to noise and low-confidence changes. Second, CARAT uses conditional score selection with regularization (Algorithm 1) to avoid systematically selecting overly conservative configurations when multiple candidates are viable.

CARAT further restricts actuation to bounded, discrete configuration spaces for both RPC and cache parameters, preventing unbounded drift and enabling repeatable behavior. Finally, CARAT follows a two-stage tuning principle: it adjusts RPC parameters periodically during I/O-active phases, while updating cache limits more conservatively at I/O boundaries.

TABLE III
HARDWARE SPECIFICATION FOR C6525-25G NODE

Component	Specification
CPU	16-core AMD 7302P at 3.00GHz
RAM	128GB ECC Memory (8x 16 GB 3200MT/s RDIMMs)
Disk	Two 480 GB 6G SATA SSD
NIC	Two dual-port 25Gb GB NIC (PCIe v4.0)

This boundary-aligned cache actuation acts as a stabilizing gate, reducing sensitivity to transient bursts and limiting interference with in-flight RPC dynamics. Together, these mechanisms allow CARAT to operate online and re-adjust promptly as conditions change, without inducing prolonged instability or persistent performance degradation.

IV. EVALUATION

A. Cluster Setup

We evaluated CARAT on the publicly available CloudLab platform [30] for reproducibility. We did not use proprietary HPC systems because CARAT’s actuation and observability require elevated privileges: updating Lustre client tunables (e.g., RPC window size, RPCs-in-flight, and client cache limits) and accessing certain client-local/low-level counters (e.g., LLITE statistics) typically requires root-level access, which is often unavailable to end users on production systems. Accordingly, we assume an administrator-managed deployment model in which CARAT runs as a system service on compute nodes (or is executed with the necessary privileges), rather than being invoked directly by individual applications.

Our testbed used ten CloudLab c6525-25g machines (Table III). We deployed Lustre 2.15.5 with one dual-purpose node as MGS+MDS, four OSS nodes (each OSS hosting two OSTs mapped to two SSD partitions), and five client nodes. Unless stated otherwise, default striping was used. Each experiment was repeated five times to account for system noise and variability.

B. Workload Setup & Data Collection

A core principle of CARAT is the creation of local metrics that effectively capture the influence of I/O patterns on the global storage system. This approach uniquely enables the training of our model using simple training data, while still achieving high accuracy when applied to more complex I/O patterns and realistic HPC executions. To validate this principle, the ML models were trained using the simplest workloads in Filebench [31]: single-stream I/O patterns (processes accessing a single file on a single OST) with varying access patterns (sequential or random) and request sizes (8 KB, 1 MB, 16 MB). We used the following naming convention to refer the used Filebench workload during evaluations: `[stream_type]_[operation_type]_[access_type]_[size]`. Here, `stream_type` indicates either single stream or five streams (*s*, *f*), `operation_type` represents either read or write (*rd*, *wr*), `access_type` denotes

TABLE IV
ERROR RATES OF ML MODELS

	Read Model	Write Model
SVM [25]	0.23	0.25
FC-NN	0.11	0.21
RNN [28]	0.17	0.23
TCN [29]	0.11	0.28
GBDT [27]	0.04	0.12

either sequential or random (*sq, rn*), and request_sizes are specified by their actual sizes (*8k, 1m, 16m*).

Training Data. To collect training data, we simulated both Read and Write operations using specified I/O patterns. Each pattern was executed for 300 seconds and repeated 30 times to generate a sufficient number of samples. During these simulations, we probed the system at half-second intervals to gather raw statistics and made random adjustments to the targeted tunable parameters after each probe. These random tuning actions caused the I/O client to experience a variety of RPC communication scenarios, allowing for a thorough evaluation of the designed metrics’ effects and providing valuable insights for the machine learning model’s training.

Evaluation Workloads. We evaluated the ML models using new, unseen constant workload, dynamically changing workloads, workloads with interferences, and real-world HPC applications.

C. ML Model Accuracy Evaluation

We trained and tuned multiple classifiers on offline data comprising 100,730 read-only and 98,078 write-only nonzero samples, split 80:20 into train/validation. We use *error rate* (i.e., $1 - \text{accuracy}$) as the metric and perform hyperparameter search for each model. Table IV summarizes results. The read/write gap reflects different operation complexity in Lustre (see § III-C).

GBDT [27] attains the lowest error for both reads (0.04) and writes (0.12), and we adopt it in CARAT. Its tree-based learning captures nonlinear feature–performance relations well on moderately sized datasets and is robust to noise and sparsity. Neural models (FC-NN, RNN, TCN) can overfit with limited data, particularly TCN on writes, while SVM underfits due to its simpler decision boundary. Beyond aggregate error, our qualitative inspection suggests the read-focused model is generally more accurate and stable than the write-focused model, which is consistent with the greater complexity and variability of write behavior in Lustre. We therefore use the learned model primarily as a lightweight filter to eliminate clearly unpromising configurations; the subsequent probability thresholding and bounded configuration space in the online tuner further reduce the impact of occasional mispredictions and prevent overly aggressive actions.

D. Tuning Evaluations

We conducted **five** sets of evaluations to validate CARAT’s tuning capabilities under diverse I/O patterns and system

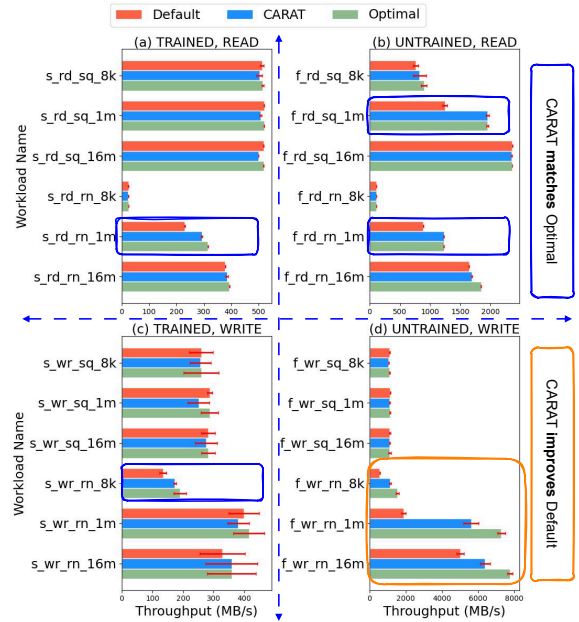


Fig. 6. Performance comparisons of tuning static workloads.

conditions, summarized as follows:

- **Static workloads:** Firstly, we assessed the CARAT to static I/O patterns. We evaluated both seen and unseen Filebench workloads to verify its effectiveness. (§IV-E).
- **Dynamic workloads:** Secondly, we demonstrated tuning adaptability of CARAT on dynamically changing I/O patterns. We evaluated how fast and how accurate CARAT reacts to the I/O pattern changes (§IV-F).
- **Independent tuning:** Thirdly, we evaluated how CARAT can make distinct tuning decisions on different I/O clients of the same applications and illustrated whether it will improve the overall I/O performance of the application (§IV-G).
- **External interference:** Fourthly, we evaluated the performance of CARAT when there are interference I/O behaviors in the global storage system, aiming to show the effectiveness of using only local metric to handle global storage system status (§IV-H).
- **Real-world applications:** Lastly, we validated CARAT tuning capabilities on real-world deep learning and HPC applications beyond benchmark workloads. (§IV-I).

E. Tuning Static Workloads

We first evaluated CARAT towards static executions of different Filebench I/O workloads (both seen and unseen I/O patterns) [31]. These evaluations focus on testing the framework’s performance to static I/O patterns. For comparison, we ran the workloads under three distinct execution scenarios: **default**, **tuning**, and **optimal**. The default scenario utilized Lustre’s default configuration. In the tuning scenario, CARAT dynamically adjusted Lustre’s configurations. The optimal scenario involved applying the best possible configuration for each workload, determined through simulations across all possible configurations offline. We executed each workload

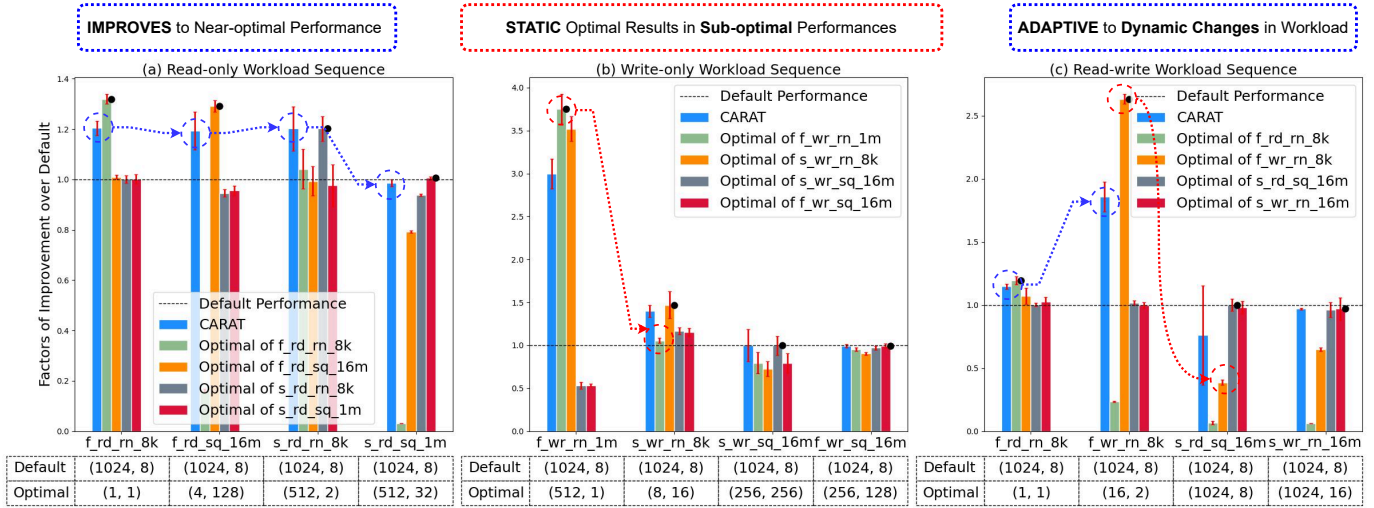


Fig. 7. Performance (throughput) comparisons of tuning dynamic workloads. Both *default* and *optimal* configurations are shown under the respective I/O patterns in the following format (‘RPC Window Size’, ‘RPCs in Flight’). The black dot represents the *optimal*.

five times, reporting the average performance alongside the standard deviation as an error bar in our visual results.

Figure 6 reports the results. In total, we evaluated 24 different I/O workloads from Filebench. The top row includes all Read workloads and the bottom row includes all Write ones. The left column includes all I/O workloads that were used during training. The right column, however, includes only those workloads that are never seen by the model. Among all the results, we highlight two cases, where *default* and *optimal* configurations have significant performance differences. Among them, the blue rectangles circle cases where CARAT matches the *optimal*; while the yellow ones circle cases where CARAT improves the *default* baseline and results in performance closer to *optimal*.

From these results, we can observe that across all workloads, CARAT either matched the performance of the *default* configuration (Baseline) within a 10% variation or significantly enhanced it, achieving up to a **3-fold** increase in performance by matching the *optimal*. The **Figure 6(d)** is exceptionally worth noting. For such an 1M write I/O pattern, traditional wisdom is to maximize RPC generation and transfer speed to send more data. However CARAT chooses to reduce RPC generation speed but delivers better performance. We checked the case and noticed that this workload contains heavy in-place updates, hence could leverage write dirty cache if the writes can be buffered in the cache longer. CARAT identifies and effectively exploits this opportunity.

F. Tuning Dynamic Workloads

We evaluated CARAT with dynamically changing I/O patterns. In this scenario, CARAT is effective because it captures the changes instantly and tunes each I/O client independently and rapidly. In these evaluations, we created dynamically changing I/O patterns by running a sequence of Filebench workloads. To be general, we explored three sequences of workloads: a sequence of various read workloads, a sequence of various write workloads, and a sequence of mixed read and

write workloads. Each sequence includes four workloads. After 300 seconds of running a particular workload, the execution would transition to the next workload.

Similar to the previous scenario, we compared both **default** and **optimal**. However, the optimal is no longer one configuration. Instead, we evaluate on optimal of each workload of the sequence. We named them based on the workload name and plots their performance individually as shown in Figure 7. Here, subplots (a, b, c) show the performance of three sequences (Read-only, Write-only, and Mixed). The four groups along the *x*-axis are the four Filebench workloads that were executed in order in the sequence. The bars show the performance of CARAT and different *optimal* configurations. They are all normalized based on the *default* configuration (1.0 in *y*-axis). Please note that CARAT is always comparing with the optimal configuration of each I/O workload.

The results clearly illustrate the CARAT’s capability and advantages to adjust continuously to the changing I/O patterns. Across all the cases, CARAT is able to adapt to the new I/O pattern and achieve near-optimal performance. We observed overall improvements up to **3×** better than the baseline for the I/O patterns in the sequence. The individual *optimal* static configurations experienced much worse performance as the I/O pattern changes.

G. Performance of Independent Tuning

We assess CARAT when an application’s processes exhibit different I/O behaviors. Table V shows two processes on a single client issuing simultaneous 8 KB sequential write (Process-1) and read (Process-2) in a file-per-process mode via different I/O clients. We compare CARAT’s online adaptation against three static choices: the Lustre default and two fixed settings (Optimal-1, Optimal-2) that correspond to the most frequently selected per-process configurations observed during tuning; tuples denote (*RPC window pages*, *RPCs in flight*). CARAT consistently delivers higher throughput for both processes, demonstrating that per-client dynamic tuning

TABLE V
INDEPENDENT TUNING EXECUTIONS

	Default (MB/s)	Optimal-1 (MB/s)	Optimal-2 (MB/s)	CARAT (MB/s)
Process-1	76.5	73.8	77.8	93.6
Process-2	14.4	25.1	26.1	58.1
Configuration	(1024, 8)	(1024, 256)	(64, 256)	Dynamic

TABLE VI
EXTERNAL INTERFERENCE EXECUTIONS

External Interference Type	Aggregated Cluster Throughput	
	Default (MB/s)	CARAT (MB/s)
All Read Workloads	1223.04	1403.80
All Write Workloads	2445.64	3604.38
Mix of Read-Write Workloads	1030.96	3057.08

outperforms static “optimal” settings as conditions evolve across co-running read/write streams.

H. Tuning under External Interference

We evaluate CARAT under server-side contention created by concurrent clients, testing whether client-local decisions generalize to shared, interfering environments. When multiple clients target overlapping OSTs, queueing rises and service rate fluctuates. Bursty writers inject many under-filled RPCs that inflate per-RPC fixed costs; competing readers see elevated per-page latency and sporadic channel idling; mixed read-write phases exacerbate head-of-line blocking and cache-pressure-induced flush spurts. We induce these effects by running five distinct workloads from five clients against overlapping OSTs in three scenarios: all-read, all-write, and mixed set of five workloads.

CARAT reacts to these conditions using only local signals: it trims in-flight concurrency when per-page RPC latency climbs and channel utilization stalls, enlarges the RPC window to reduce small-RPC bursts once contention appears, and on write-heavy paths, raises dirty-cache headroom for active clients to preserve coalescing while keeping inactive ones at minimal cache. As contention eases, it restores concurrency to re-expose parallelism. This combination suppresses premature dispatch, stabilizes channel utilization, and smooths server queues without global coordination, improving aggregate efficiency across clients. As shown in Table VI, aggregate cluster throughput improves over the default by **15%** (all-read), **1.47×** (all-write), and up to **3.0×** (mixed), reflecting better extent filling, right-sized concurrency, and adaptive cache allocation under interference.

I. Tuning Real-world Applications

We evaluate CARAT on real applications to test generalization beyond its benchmark-trained models, covering both emerging deep learning (DL) workloads and traditional HPC applications. Importantly, these application traces and kernels are not used in training; thus, this experiment evaluates whether the client-local metrics captured by CARAT can guide tuning decisions

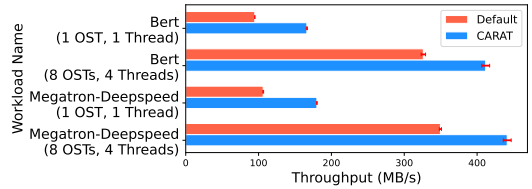


Fig. 8. DL I/O kernels (BERT [33], Megatron/DeepSpeed [34, 35]) via DLIO [32]: throughput vs. default.

TABLE VII
HPC SCIENTIFIC APPLICATION EXECUTIONS

Scientific HPC Applications	Default(MB/s)	CARAT(MB/s)
VPIC-IO (3D array write)	459.7	514.6
BDCATS-IO (3D array read)	398.2	405.3

even when the exact application access pattern was not seen during offline model construction.

DL workloads pose distinctive I/O behaviors that challenge traditional tuning [1]. Modern DL training is dominated by small, sample-oriented reads spread over numerous files, plus per-epoch shuffling and multi-threaded prefetch that create short, bursty I/O phases. These traits fragment RPC extents, trigger under-filled requests, and intermittently overwhelm or idle RPC channels. Using DLIO [32], we evaluate BERT [33] and Megatron with DeepSpeed [34, 35] across varying OST utilization and thread counts. CARAT adapts the RPC window to sustain channel utilization under small/unaligned reads, tempers in-flight concurrency under momentary contention, and raises dirty-cache headroom to coalesce bursts. This behavior is consistent with the design goal of filtering out low-confidence changes and operating within a bounded configuration space: rather than continuously exploring, CARAT applies only high-confidence adjustments that improve the likelihood of maintaining steady effective concurrency during bursty phases. In our DLIO runs, this combination reduced premature small-RPCs during bursts and preserved coalescing when sequential access emerged, enabling the observed **up to 1.75×** speedup over the default as shown in Fig. 8. Since the total data volume is fixed per run, these throughput gains translate into corresponding reductions in the I/O phase time for the DL kernels.

For traditional HPC, we use H5bench [36]: VPIC-IO (write) derived from a particle-physics code [4] and BDCATS-IO (read) based on a big-data clustering workflow. Table VII shows CARAT is on-par or better than default, confirming applicability to classic scientific workloads. We note that improvements on these kernels can be smaller than on DLIO because their I/O behavior is more sequential and regular, for which the Lustre client default RPC and caching settings are often already near-optimal. As a result, there is limited headroom for additional gains from client-side tuning; in these cases, CARAT typically either makes minor adjustments when it identifies a clear opportunity or remains close to the default settings.

TABLE VIII
CARAT OVERHEADS PER I/O CLIENT

Operation Type	Snapshot Creation Time (ms)	Inference Time (ms)	End-to-end Tuning Time (ms)
Read	0.33	10.06	24.64
Write	0.85	13.51	28.82

J. CARAT Overhead

CARAT runs independently per client, maintains only two in-memory snapshots, and collects client-local statistics without issuing remote I/O, thereby avoiding extra PFS or network traffic. At runtime, each client executes the same control loop locally: it probes metrics, selects the appropriate (read- or write-focused) model based on the observed I/O mix for that interval, performs inference once (i.e., it does not run both models), and applies an update only when the candidate passes the probability threshold; otherwise it retains the current setting.

Table VIII reports per-client averages (CloudLab) for snapshot creation, model inference, and end-to-end tuning (inference + selection + apply) under read- and write-centric workloads. Probing, inference, and tuning execute in parallel across clients, so overhead does not grow with ranks/clients/nodes, demonstrating strong scalability. This addresses the concern that frequent invocation could amplify overhead at scale: the overhead is incurred independently per client and does not introduce centralized bottlenecks. Moreover, the end-to-end tuning cost reported in Table VIII remains well below the probing period used in our experiments, leaving slack for stable operation even when tuning is evaluated frequently.

We used a short 0.5 s probing interval made possible due to usage of local-only metrics; this interval is user-configurable. The probing interval presents a responsiveness–stability tradeoff: shorter intervals can react more quickly to phase changes, while longer intervals reduce control-loop activity and further damp sensitivity to transient variations. In practice, CARAT can be run at coarser intervals for less I/O-intensive workloads or when a more conservative tuning cadence is desired.

V. RELATED WORK

Auto-tuning for HPC I/O spans a large, coupled search space and is algorithmically hard [37, 38]. Prior systems therefore adopt approximations along two main lines.

Heuristic/Rule-based tuning. Rule-driven methods encode expert knowledge or lightweight policies for specific knobs and patterns. Li et al. [39] propose a rule-based strategy; TAPP-IO [40] and DCA-IO [41] tune Lustre striping (size/count) using heuristic and log-informed rules, and IOPathTune [7] exploits client-side metrics for adaptive tuning. While efficient, such approaches struggle to generalize across diverse and time-varying I/O behaviors, and often lack a mechanism-aware way to reconcile RPC coalescing, concurrency, and cache pressure that arise prominently in PFS clients.

Black-box optimization and learning. A complementary line that models performance and searches configurations with

black-box optimizers. Cao et al. [42] compare auto-tuning strategies across file systems; SAPPHERE [43] applies Bayesian optimization; Behzad et al. [11] couple nonlinear regression with genetic algorithms. Recent systems like CAPES [15], AIOC2 [16], and Magpie [20] use DRL to learn end-to-end policies. These methods can be effective but typically depend on global instrumentation and aggregation, incurring nontrivial data-collection, training, and coordination overheads that impede online, per-client adaptation at scale.

Positioning of CARAT. In contrast, CARAT narrows the scope to *client-local* observability and actuation. It uses low-level metrics that directly reflect RPC extent utilization, in-flight concurrency, and dirty-cache dynamics, and applies lightweight ML to make online decisions per client without central coordination. This design sidesteps global telemetry cost while addressing the core client-side trade-offs that prior heuristics and global black-box methods only indirectly capture, enabling scalable RPC+cache co-tuning under dynamic workloads.

VI. CONCLUSION AND FUTURE PLAN

We presented CARAT, a ML-guided system for *client-side RPC and cache co-tuning* that operates online using only client-local signals. CARAT decouples fast-acting RPC control from slower cache-limit adjustments via a two-stage tuning, and selects configurations with a conditional score–greedy policy informed by lightweight ML models. Implemented atop Lustre, CARAT improves throughput by up to $3\times$ across benchmarks and real applications (DLIO kernels, H5bench), while incurring negligible per-client overhead and requiring no application changes or cluster-wide coordination. Our results indicate that client-side observability and actuation can effectively manage extent underutilization, congestion, and cache pressure in production-style settings. In future, we plan to broaden the tunable surface (e.g., additional client/runtime knobs) and extend the approach to metadata paths and other RPC-based PFSes. We believe this direction enables more scalable, timely, and tunable storage for data-intensive HPC workloads.

ACKNOWLEDGMENTS

We sincerely thank the reviewers for their valuable feedback. We further thank Xinyi Li and Youbiao He for their early contribution in ML models evaluation. This work was supported in part by the National Science Foundation (NSF) under grants CNS-2008265 and CCF-2412345. This effort was also supported in part by the U.S. Department of Energy (DOE) through the Office of Advanced Scientific Computing Research’s “Orchestration for Distributed & Data-Intensive Scientific Exploration” and the “Decentralized data mesh for autonomous materials synthesis” AT SCALE LDRD at Pacific Northwest National Laboratory. PNNL is operated by Battelle for the DOE under Contract DE-AC05-76RL01830. The Authors acknowledge the National Artificial Intelligence Research Resource (NAIRR) Pilot for contributing to this research result. The authors acknowledge the assistance of ChatGPT and Claude (Anthropic) in performing editorial revisions to the manuscript.

REFERENCES

- [1] Noah Lewis, Jean Luca Bez, and Surendra Byna. I/o in machine learning applications on hpc systems: A 360-degree survey. *ACM Computing Surveys*, 2025.
- [2] Hammad Ather. Parallel i/o characterization and optimization on large-scale hpc systems: A 360-degree survey. *arXiv.org*, 2024. doi: 10.48550/ARXIV.2501.00203.
- [3] Jean Luca Bez, Suren Byna, and Shadi Ibrahim. I/o access patterns in hpc applications: A 360-degree survey. *ACM Computing Surveys*, 56(2):1–41, 2023.
- [4] Surendra Byna, Jerry Chou, Oliver Rubel, Homa Karimabadi, William S Daughter, Vadim Roytershteyn, E Wes Bethel, Mark Howison, Ke-Jou Hsu, Kuan-Wu Lin, et al. Parallel i/o, analysis, and visualization of a trillion particle simulation. In *SC’12: Proceedings of the International Conference on High Performance Computing, Networking, Storage and Analysis*, pages 1–12. IEEE, 2012.
- [5] Laura Clarke, Xiangqun Zheng-Bradley, Richard Smith, Eugene Kulesha, Chunlin Xiao, Iliana Toneva, Brendan Vaughan, Don Preuss, Rasko Leinonen, Martin Shumway, et al. The 1000 genomes project: data management and community access. *Nature methods*, 2012.
- [6] Md Hasanur Rashid and Dong Dai. Adaptbf: Decentralized bandwidth control via adaptive token borrowing for hpc storage. In *2025 IEEE International Parallel and Distributed Processing Symposium (IPDPS)*, pages 775–788. IEEE, 2025.
- [7] Md Hasanur Rashid, Youbiao He, Forrest Sheng Bao, and Dong Dai. Iopathtune: Adaptive online parameter tuning for parallel file system i/o path. *arXiv preprint arXiv:2301.06622*, 2023.
- [8] Md Hasanur Rashid, Xinyi Li, Youbiao He, Forrest Sheng Bao, and Dong Dai. Dial: Decentralized i/o autotuning via learned client-side local metrics for parallel file system. In *2025 IEEE 25th International Symposium on Cluster, Cloud and Internet Computing (CCGrid)*, pages 01–04. IEEE, 2025.
- [9] Chris Egersdoerfer, Philip Carns, Shane Snyder, Robert Ross, and Dong Dai. Stellar: Storage tuning engine leveraging llm autonomous reasoning for high performance parallel file systems. In *Proceedings of the International Conference for High Performance Computing, Networking, Storage and Analysis*, pages 1252–1266, 2025.
- [10] Jean Luca Bez, Houjun Tang, Bing Xie, David Williams-Young, Rob Latham, Rob Ross, Sarp Oral, and Suren Byna. I/o bottleneck detection and tuning: Connecting the dots using interactive log analysis. In *2021 IEEE/ACM Sixth International Parallel Data Systems Workshop (PDSW)*, pages 15–22. IEEE, 2021.
- [11] Babak Behzad, Surendra Byna, and Marc Snir. Optimizing i/o performance of hpc applications with autotuning. *ACM Transactions on Parallel Computing (TOPC)*, 5(4):1–27, 2019.
- [12] Megha Agarwal, Divyansh Singhvi, Preeti Malakar, and Suren Byna. Active learning-based automatic tuning and prediction of parallel i/o performance. In *2019 IEEE/ACM Fourth International Parallel Data Systems Workshop (PDSW)*, pages 20–29. IEEE, 2019.
- [13] Ayşe Bağbaba, Xuan Wang, Christoph Niethammer, and José Gracia. Improving the i/o performance of applications with predictive modeling based auto-tuning. In *2021 International Conference on Engineering and Emerging Technologies (ICEET)*, pages 1–6. IEEE, 2021.
- [14] Zhangyu Liu, Cheng Zhang, Huijun Wu, Jianbin Fang, Lin Peng, Guixin Ye, and Zhanyong Tang. Optimizing hpc i/o performance with regression analysis and ensemble learning. In *2023 IEEE International Conference on Cluster Computing (CLUSTER)*, pages 234–246. IEEE, 2023.
- [15] Yan Li, Kenneth Chang, Oceane Bel, Ethan L Miller, and Darrell DE Long. Capes: Unsupervised storage performance tuning using neural network-based deep reinforcement learning. In *Proceedings of the international conference for high performance computing, networking, storage and analysis*, pages 1–14, 2017.
- [16] Wen Cheng, Shijun Deng, Lingfang Zeng, Yang Wang, and André Brinkmann. Aioc2: A deep q-learning approach to autonomic i/o congestion control in lustre. *Parallel Computing*, 108:102855, 2021.
- [17] Chris Egersdoerfer, Md Hasanur Rashid, Dong Dai, Bo Fang, and Tallent Nathan. Understanding and predicting cross-application i/o interference in hpc storage systems. In *SC24-W: Workshops of the International Conference for High Performance Computing, Networking, Storage and Analysis*, pages 1330–1339. IEEE, 2024.
- [18] Mihailo Isakov, Mikaela Currier, Eliakin Del Rosario, Sandeep Madireddy, Prasanna Balaprakash, Philip Carns, Robert B Ross, Glenn K Lockwood, and Michel A Kinsy. A taxonomy of error sources in hpc i/o machine learning models. In *SC22: International Conference for High Performance Computing, Networking, Storage and Analysis*, pages 01–14. IEEE, 2022.
- [19] Chris Egersdoerfer, Arnav Sareen, Jean Luca Bez, Suren Byna, Dongkuan DK Xu, and Dong Dai. Ioagent: Democratizing trustworthy hpc i/o performance diagnosis capability via llms. In *2025 IEEE International Parallel and Distributed Processing Symposium (IPDPS)*, pages 322–334. IEEE, 2025.
- [20] Houkun Zhu, Dominik Scheinert, Lauritz Thamsen, Kordian Gontarska, and Odej Kao. Magpie: Automatically tuning static parameters for distributed file systems using deep reinforcement learning. In *2022 IEEE International Conference on Cloud Engineering (IC2E)*, pages 150–159. IEEE, 2022.
- [21] Kai Lu, Guokuan Li, Jiguang Wan, Ruixiang Ma, and Wei Zhao. Adsts: Automatic distributed storage tuning system using deep reinforcement learning. In *Proceedings of the 51st International Conference on Parallel Processing*, pages 1–13, 2022.
- [22] Jiaxin Dong, Md Hasanur Rashid, Helen Xu, and Dong

- Dai. RL4sys: A lightweight system-driven rl framework for drop-in integration in system optimization. In *Proceedings of the SC'25 Workshops of the International Conference for High Performance Computing, Networking, Storage and Analysis*, pages 1406–1414, 2025.
- [23] U. Plechschmidt. It’s lonely at the top: Lustre continues to dominate top 100 fastest supercomputers. URL <https://community.hpe.com/t5/Advantage-EX/It-s-lonely-at-the-top-Lustre-continues-to-dominate-top-100/ba-p/7109668>.
- [24] Spencer Shepler, Brent Callaghan, David Robinson, Robert Thurlow, Carl Beame, Mike Eisler, and David Noveck. Network file system (nfs) version 4 protocol. Technical report, 2003.
- [25] Corinna Cortes and Vladimir Vapnik. Support-vector networks. *Machine learning*, 20(3):273–297, 1995.
- [26] Warren S McCulloch and Walter Pitts. A logical calculus of the ideas immanent in nervous activity. *The bulletin of mathematical biophysics*, 5(4):115–133, 1943.
- [27] Jerome H Friedman. Greedy function approximation: a gradient boosting machine. *Annals of statistics*, pages 1189–1232, 2001.
- [28] David E Rumelhart, Geoffrey E Hinton, and Ronald J Williams. Learning internal representations by error propagation, parallel distributed processing, explorations in the microstructure of cognition, ed. de rumelhart and j. mcclelland. vol. 1. 1986. *Biometrika*, 71:599–607, 1986.
- [29] Shaojie Bai, J Zico Kolter, and Vladlen Koltun. An empirical evaluation of generic convolutional and recurrent networks for sequence modeling. *arXiv preprint arXiv:1803.01271*, 2018.
- [30] Dmitry Duplyakin, Robert Ricci, Aleksander Maricq, Gary Wong, Jonathon Duerig, Eric Eide, Leigh Stoller, Mike Hibler, David Johnson, Kirk Webb, et al. The design and operation of {CloudLab}. In *2019 USENIX annual technical conference (USENIX ATC 19)*, pages 1–14, 2019.
- [31] Vasily Tarasov, Erez Zadok, and Spencer Shepler. Filebench: A flexible framework for file system benchmarking. *USENIX; login*, 41(1):6–12, 2016.
- [32] Hariharan Devarajan, Huihuo Zheng, Anthony Kougkas, Xian-He Sun, and Venkatram Vishwanath. Dlio: A data-centric benchmark for scientific deep learning applications. In *2021 IEEE/ACM 21st International Symposium on Cluster, Cloud and Internet Computing (CCGrid)*, pages 81–91. IEEE, 2021.
- [33] Jacob Devlin, Ming-Wei Chang, Kenton Lee, and Kristina Toutanova. Bert: Pre-training of deep bidirectional transformers for language understanding. *arXiv preprint arXiv:1810.04805*, 2018.
- [34] Mohammad Shoeybi, Mostofa Patwary, Raul Puri, Patrick LeGresley, Jared Casper, and Bryan Catanzaro. Megatron-lm: Training multi-billion parameter language models using model parallelism. *arXiv preprint arXiv:1909.08053*, 2019.
- [35] Jeff Rasley, Samyam Rajbhandari, Olatunji Ruwase, and Yuxiong He. Deepspeed: System optimizations enable training deep learning models with over 100 billion parameters. In *Proceedings of the 26th ACM SIGKDD International Conference on Knowledge Discovery & Data Mining*, pages 3505–3506, 2020.
- [36] Tonglin Li, Suren Byna, Quincey Koziol, Houjun Tang, Jean Luca Bez, and Qiao Kang. h5bench: HDF5 I/O Kernel Suite for Exercising HPC I/O Patterns. In *Proceedings of Cray User Group Meeting, CUG 2021*, 2021.
- [37] Matthieu Dorier, Romain Egele, Prasanna Balaprakash, Jaehoon Koo, Sandeep Madireddy, Srinivasan Ramesh, Allen D Malony, and Rob Ross. Hpc storage service auto-tuning using variational-autoencoder-guided asynchronous bayesian optimization. In *2022 IEEE International Conference on Cluster Computing (CLUSTER)*, pages 381–393. IEEE, 2022.
- [38] Daniel S Bernstein, Robert Givan, Neil Immerman, and Shlomo Zilberstein. The complexity of decentralized control of markov decision processes. *Mathematics of operations research*, 27(4):819–840, 2002.
- [39] Yan Li, Xiaoyuan Lu, Ethan L Miller, and Darrell DE Long. Ascar: Automating contention management for high-performance storage systems. In *2015 31st Symposium on Mass Storage Systems and Technologies (MSST)*, pages 1–16. IEEE, 2015.
- [40] Sarah Neuwirth, Feiyi Wang, Sarp Oral, and Ulrich Bruening. Automatic and transparent resource contention mitigation for improving large-scale parallel file system performance. In *2017 IEEE 23rd International Conference on Parallel and Distributed Systems (ICPADS)*, pages 604–613. IEEE, 2017.
- [41] Sunggon Kim, Alex Sim, Kesheng Wu, Suren Byna, Teng Wang, Yongseok Son, and Hyeonsang Eom. Dca-io: A dynamic i/o control scheme for parallel and distributed file systems. In *2019 19th IEEE/ACM International Symposium on Cluster, Cloud and Grid Computing (CCGRID)*, pages 351–360. IEEE, 2019.
- [42] Zhen Cao, Vasily Tarasov, Sachin Tiwari, and Erez Zadok. Towards better understanding of black-box {Auto-Tuning}: A comparative analysis for storage systems. In *2018 USENIX Annual Technical Conference (USENIX ATC 18)*, pages 893–907, 2018.
- [43] Wenhao Lyu, Youyou Lu, Jiwu Shu, and Wei Zhao. Sapphire: Automatic configuration recommendation for distributed storage systems. *arXiv preprint arXiv:2007.03220*, 2020.